

## Are Phase Center Corrections identical for identical frequencies from different GNSS?

Johannes KRÖGER, Yannick BREVA, Tobias KERSTEN, and Steffen SCHÖN,  
Germany

**Key words:** antenna calibration, phase center corrections, Multi-GNSS, Beidou

### SUMMARY

Global Navigation Satellite Systems (GNSS) are used for the realization of land and water management tasks since they provide an absolute and highly accurate position. Especially measurements for the reorganization of land parcels are often carried out in dense urban areas. In these situations, only multi-GNSS enables a reliable position solution. In less severe situations, it improves the accuracy of the position significantly. The quality of multi-GNSS carrier phase measurements depends, among other factors, on the knowledge of the exact electrical receiving point of the receiver antenna, known as phase center. This location varies with the direction of the incoming signal, so that phase center corrections (PCC), including a phase center offset (PCO) and phase center variations (PCV), have to be taken into account. These corrections are frequency and antenna type dependent with the result that PCC for each antenna type and frequency have to be determined separately. This is especially true for including newer frequencies (e.g. L5) or GNSS like Galileo or Beidou.

In this contribution, the theoretical background of PCC and a short description of our estimation process developed at the Institut für Erdmessung (IfE) are given. Next, the repeatability of different calibrations for the same antenna is assessed. The results underline an overall good repeatability for several GPS, Galileo and Beidou frequencies with differences at maximum of 2 mm at low elevations except for L2 frequencies of GPS. Here, the differences are maximal 3 mm, probably due to settings of the tracking loop parameters. The comparison of PCC of identical frequencies from different GNSS shows a very good agreement between GPS and Galileo L1 and L5 frequencies. Here, the maximum difference is less than 1 mm. The differences between Galileo L7 (E5b) and Beidou L7 (B2b) are clearly larger, at maximum 2.3 mm. The significantly different number of observations for the PCC estimation could explain these deviations.

In a joint estimation approach, the identical frequencies of different GNSS are combined at the normal equation level. The jointly estimated PCC are compared to the “classical” approach resulting in differences smaller than 1.5 mm. Moreover, it could be shown, that these differences are mainly linked to the number of observations from each individual frequency. Since other antenna-receiver combinations show higher differences, a bigger study with several, different combinations need to be carried out in near future.

# Are Phase Center corrections identical for identical frequencies from different GNSS?

Johannes KRÖGER, Yannick BREVA, Tobias KERSTEN and Steffen SCHÖN,  
Germany

## 1. Introduction

Precise positions are needed for the realization of land and water management tasks, e.g. for the reorganization of land parcels or the construction of water reservoirs. Global Navigation Satellite Systems (GNSS) cannot only be used for precise positioning, navigation and timing (PNT) but also for establishing of terrestrial reference frames for geospatial tasks (Altamimi, et al., 2016), e.g. to document the ramifications of climate change. Moreover, GNSS allows accurate monitoring at a local scale, such as of landslides (Schön, 2007) or sinkholes in urban areas (Kersten, et al., 2017). Especially in dense urban areas, the satellite visibility is challenging. Multi-GNSS processing increases not only the number of epochs where a position solution can be computed but also improves the accuracy of the position solution due to a significantly better satellite geometry (Odolinski & Teunissen, 2015).

To get the precise coordinates of a marker in a global or local frame, the antenna height has to be measured. This is typically done by determining the offset vector between the marker and a physically accessible point at the antenna, the so-called antenna reference point (ARP). Often, this is the substructure of the antenna. However, the actual phase measurement itself refers to the electrical carrier phase center, not directly accessible by geometric measurements.

Therefore, the quality of GNSS phase measurements depends, among other factors, on the knowledge of the exact electrical receiving point of the GNSS receiver antenna. To this end, frequency and antenna dependent phase center corrections (PCC) are determined so that the corrections between the ARP and the phase center can be applied to the measurements. Since multi-GNSS is a key factor nowadays, PCC for newer frequencies like GPS L5 and recently established GNSS such as Galileo and Beidou have to be determined and provided to the user in order to take the benefits from multi-GNSS measurements.

PCC consist of a 3D offset vector pointing from the ARP to the electrical phase center, the so-called phase center offset (PCO), and corresponding phase center variations (PCV). These PCV are azimuthal and elevation-dependent, since the pattern of the GNSS receiver antennas deviate from an ideal omnidirectional radiator as they are a compromise of several physical parameters (e.g. gain, multipath reduction, weight and size, etc.) (Rao, et al., 2013; Stutzman & Thiele, 2012).

In order to get the complete set of PCC, the PCO vector  $PCO$  is projected onto the unit line-of-sight vector  $\vec{e}$  pointing from the receiver to the satellite  $k$  which is parameterized by the azimuth angle  $\alpha^k$  and the zenith angle  $z^k$ . The PCV are gridded with respect to azimuth and zenith angle, typically in steps of  $5^\circ$ , respectively. Due to the relative character of GNSS observations, a constant part  $r$  is also present which cannot be separated from the receiver clock error so that a datum constraint is required to solve the rank defect.

$$PCC(\alpha, z) = -PCO \cdot \vec{e}(\alpha^k, z^k) + PCV(\alpha^k, z^k) + r. \quad (1)$$

Usually, the datum definition is either done by restricting the PCV in zenith to zero or by setting up a zero mean condition over parts or over the whole hemisphere.

State of the art antenna calibration determines the PCC either in an anechoic chamber using artificial generated signals (Görres, et al., 2006; Zeimet & Kuhlmann, 2008; Becker, et al., 2010) or in the field using a precisely calibrated robot and real satellite signals (Menge, et al., 1998; Wübbena, et al., 2000; Böder, et al., 2001; Seeber & Böder, 2002; Wübbena, et al., 2019; Kröger, et al., 2020a; Willi, et al., 2020).

At the Institut für Edmessung (IfE), PCC are obtained by an absolute calibration in the field using a robot, which precisely rotates and tilts the antenna under test (AUT) around a randomly chosen but fixed point in space, see Figure 1. At a nearby located reference station and the robot station, GNSS raw data are recorded using identical geodetic receivers. Additionally, the robot poses are logged so that the actual position of the AUT can be computed in a post processing approach by use of a robot model with its defined arm lengths (Kersten, 2014).

Based on the corrected position of the AUT and the data of the reference station, time-differenced receiver-to-receiver single differences (dSD) are calculated so that the final observations only contain the PCC of the AUT and noise. All other error sources are either cancelled out on the short baseline configuration or modelled.

Next, the dSD serves as input in a least-squares adjustment for estimating the PCC. Here, the PCC are parametrized by spherical harmonics (SH) which estimated coefficients are subsequently used in a SH synthesis in order to get grid values in 5° azimuth and 5° elevation steps for the PCV as well as the PCO vector. This information is then written in the Antenna Exchange format (ANTEX) (Rothacher & Schmid, 2010). A detailed description of the calibration method and the PCC estimation algorithm used at the IfE are described in Kröger et al. (2020a) and Kröger et al. (2021).

This contribution is structured as follows. Section 2 presents the repeatability of estimated PCC for several GPS, Galileo and Beidou frequencies. Next, in Section 3 the differences between PCC of identical frequencies but from different GNSS are analyzed. Consequently, in Section 4 PCC of identical frequencies but from different GNSS are computed in a joint estimation approach including an analysis with balanced number of observations per 5° elevation bin. The paper closes with the conclusion given in Section 5.

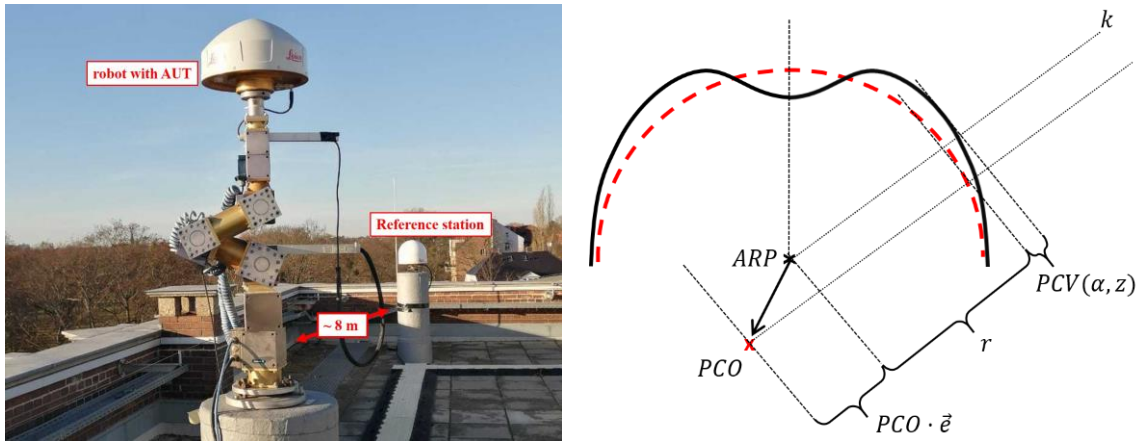


Figure 1: Calibration set up at the IfE (left) and the sketch of PCC geometry, containing the PCO, PCV and the constant part  $r$  (right).

## 2. Repeatability of calibration results

In order to assess the repeatability of our estimated PCC, several calibrations have been carried out in April 2020. In this contribution, the estimated PCC of two individual sets are compared. To ensure that the calibration results are independent of the center of rotation, the fixed point in space has been shifted by 2 cm before one of the calibrations.

Here, the repeatability of estimated PCC for a geodetic reference choke ring antenna with a radome, namely LEIAR20 LEIM (see Figure 1 on the robot) between DOY105 and DOY107 (2020) is shown. During the calibrations Septentrio PolaRx5TR receivers were used at each station.

When different PCC are compared, it is important to take the whole PCC set into account consisting of the PCO and the PCV. If the PCV from different sets of PCC should be analysed separately, the PCC have to be related to a common PCO set (Menge, et al., 1998). In this contribution, the whole PCC sets are compared by applying Equation 1. In order to consider the rank defect of the PCC and for a better visualisation, the individual PCC are constrained to zero in zenith before the PCC differences ( $\Delta PCC$ ) are calculated.

Due to the fact that the datum definition of individual  $PCC_i$  are generally not reported, a simple datum transformation cannot be applied. Therefore, Schön & Kersten (2013) propose different comparison strategies like the datum independent spread  $\Delta s$

$$\Delta s = (PCC_{1_{max}} - PCC_{1_{min}}) - (PCC_{2_{max}} - PCC_{2_{min}}) \quad (2)$$

Figure 2 presents the repeatability of the calibration for GPS frequencies in a cumulative histogram taking the azimuthal and elevation-dependent variations into account. It can be seen that 95% of the GL1C and GL5Q PCC differences are smaller than 0.71 mm and 0.96 mm, respectively. For GL2L and GL2W the differences are at maximum 3 mm. On the right side of Figure 2, only elevation-dependent differences are shown by computing the mean difference over the whole azimuthal range. Here, it can be seen that principally larger

differences up to 2.5 mm are present at low elevations. However, for GL2W high differences also occur in mid elevation ranges, i.e. 50° to 70°. This could be related to the used tracking algorithm settings since the parameters for the bandwidth, the delay-locked loops (DDL) as well as the phase-locked loop (PLL) have an impact on the estimation of PCC (Kersten, 2014). Thus, this issue needs further investigations, especially due to the fact that every receiver processes the phase measurements differently. Particularly, this is the cases for the encrypted P-Code of GPS, i.e. GL2W.

Figure 3 depicts the repeatability of various Galileo frequencies. The maximal difference for all frequencies is smaller than 2 mm if azimuthal and elevation-dependent PCC are taken into account. The repeatability is better than 1 mm, even at low elevations, if only elevation-dependent variations are considered. This underlines a high repeatability between individual calibrations.

Figure 4 shows the repeatability of estimated Beidou frequencies. The repeatability is comparable to those of Galileo frequencies, even though the only elevation-dependent  $\Delta$ PCC are slightly higher for CL2I and CL6I. They reach a magnitude of almost 1.2 mm.

Table 1 summarizes the difference spread  $\Delta$ s and the differences of the root mean square (RMS) between the estimated PCC of DOY105 and DOY107 (2020). These measures underline the visualised results given Figure 2, Figure 3 and Figure 4.

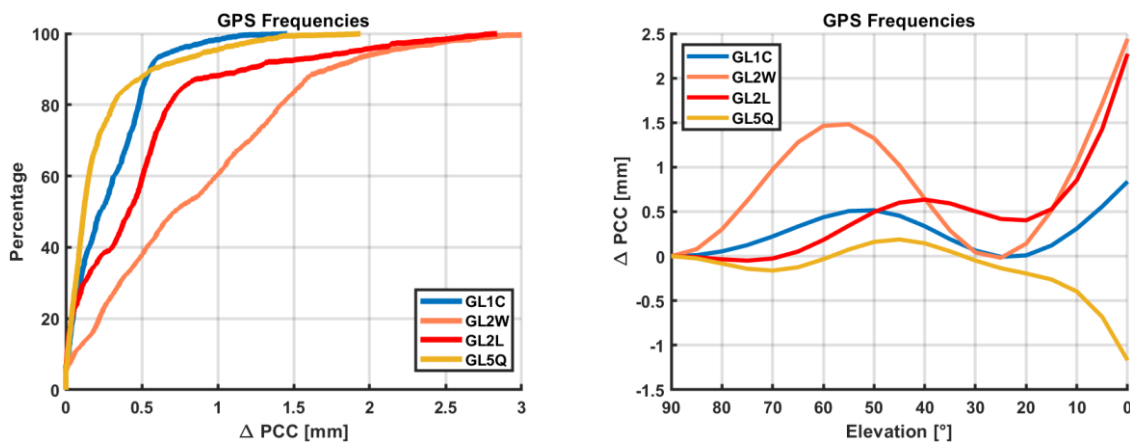


Figure 2:  $\Delta$ PCC between two calibrations of the same antenna (LEIAR20 LEIM) for GPS frequencies.

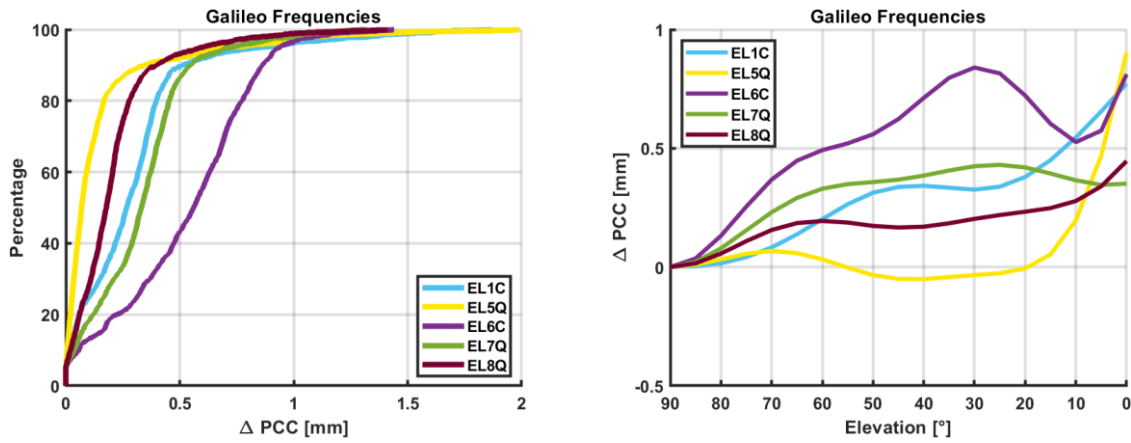


Figure 3:  $\Delta PCC$  between two calibrations of the same antenna (LEIAR20 LEIM) for Galileo frequencies.

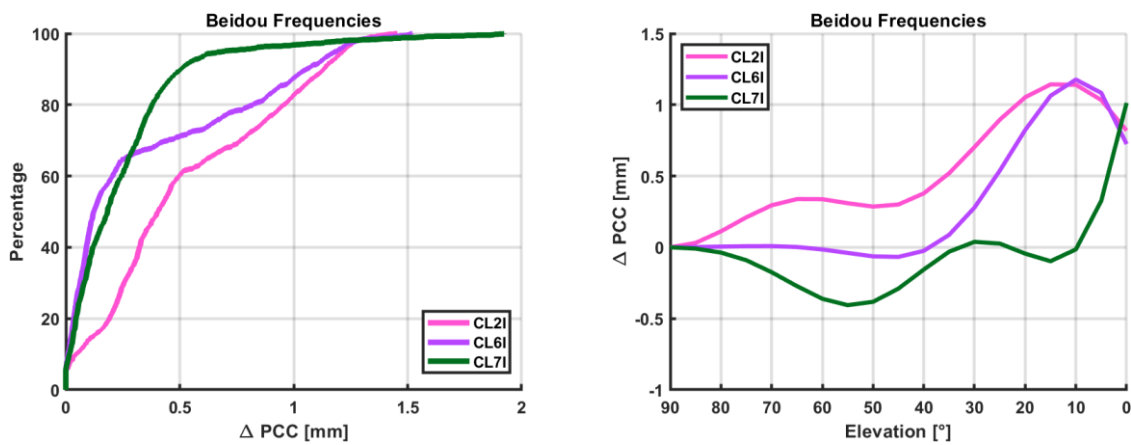


Figure 4:  $\Delta PCC$  between two calibrations of the same antenna (LEIAR20 LEIM) for Beidou frequencies.

Table 1: Repeatability of antenna calibration characterized by  $\Delta s$  (spread) and  $\Delta RMS$  of the PCC for LEIAR20 LEIM between two calibrations on DOY105 and DOY107 (2020)

Frequency	$\Delta s$ [mm]	$\Delta RMS$ [mm]
GL1C	0.96	0.37
GL2W	2.14	1.08
GL2L	2.08	0.75
GL5Q	1.40	0.38
EL1C	1.72	0.41
EL5Q	1.58	0.31
EL6C	1.37	0.60
EL7Q	0.40	0.39
EL8Q	0.84	0.29
CL2I	0.99	0.65
CL6I	1.18	0.54
CL7I	0.97	0.38

### 3. Comparison of PCC for identical frequencies from different GNSS

Theoretically, PCC are frequency-dependent. Consequently, we could assume that it is sufficient to provide one set of PCC for the identical frequencies from different GNSS (e.g. GL1C and EL1C). However, geodetic receivers process phase measurements from different GNSS to some extent differently. This includes the code or signal part used to determine the carrier phase as well as the tracking loop parameters. This is one of the reasons for existing phase biases in multi-GNSS processing (Håkansson, et al., 2017), which could lead to higher  $\Delta$ PCC of identical frequencies from different GNSS.

Figure 5 represents the different frequencies of GPS, Galileo and Beidou. Note, that the x-axis is not continuously in the range between 1300 MHz and 1550 MHz. Both, the specification for the frequency band (black) and the RINEX observation code (blue, neglecting the tracking mode or channel) is provided (IGS, 2018). Frequencies indicated by a red dot are covered within this contribution since they can be tracked with the used Septentrio receivers. It can be seen, that in total the  $\Delta$ PCC of three frequency bands of different GNSS can be analysed: L1 and L5 for GPS and Galileo as well as L7 for Galileo and Beidou.

When PCC of signals from different GNSS but also identical frequencies from the same system (e.g. GL2W and GL2L) are compared, it is important to consider the code structure of the respective signal since this specifies how the signals are tracked and processed by the receiver. Table 2 summarizes the signal characteristics for the identical frequencies that are analysed in the following. Most codes are modulated using binary phase shift keying (BPSK) except L5, which is modulated by quadrature phase shift keying (QPSK) and E1 by composite binary offset carrier (CBOC) (Kaplan & Hegarty, 2017). The different modulations as well as the code length may be treated differently from different receivers. A special focus should be placed on the encrypted P-Code of GPS (GL2W) since it is decoded by proprietary algorithms.

Figure 6 depicts the  $\Delta$ PCC of identical frequencies but different GNSS. It can be clearly seen that the PCC of the L1 and L5 frequencies of GPS and Galileo match well since the differences are smaller than 1 mm. Higher differences occur between the L7 frequencies of Galileo and Beidou. Here, differences at maximum of 2.3 mm are visible. This can be

Table 2: Characteristics of L1, L2, L5 and L7 signals for GPS, Galileo and Beidou (Kaplan & Hegarty, 2017).

Frequency band	RINEX specificator	Frequency [MHz]	Modulation	Code length [chips]	Repetition time
L1	GL1C	1575.42	BPSK	1 023	1 ms
L2 (P)	GL2W	1227.60	BPSK	$6.1871 \cdot 10^{12}$	7 days
L2 (L)	GL2L		BPSK	767 250	1.5 s
L5 (Q)	GL5Q	1176.45	QPSK	10 230	1 ms
E1	EL1Q	1575.42	CBOC	4 092	4 ms
E5a	EL5Q	1176.45	BPSK	10 230	1 ms
E5b	EL7Q	1207.14	BPSK	10 230	1 ms
B2b	CL7I	1207.14	BPSK	2 046	2 ms

explained by the significantly different number of available observations, see Figure 7 (DOY105). All in all, there are more than 26 000 observations more for EL7Q compared to CL7I. Note, that for these analyses a significantly longer calibration was carried out in order to get a sufficient number of Beidou observations. For a standard GPS and Galileo calibration less than 50 000 GL1C and about 35 000 Galileo observations are usually used.

Moreover, Figure 6 shows  $\Delta$ PCC of two GPS signals on the identical frequency (1227.60 MHz) but with a different tracking mode: GL2W and GL2L. In this case one would expect that the differences are below the millimeter-level since no phase bias between different GNSS are present. However, in this antenna-receiver combination the  $\Delta$ PCC reach a maximum of 4.2 mm. On the one hand, the larger differences can be explained again by the different number of observations. This issue will be investigated in the next section. On the other hand, receiver settings may have an impact.

All in all, the results presented here are only valid for this specific antenna-receiver combination. In another combination higher differences between identical frequencies but different GNSS already have been detected. Kröger et al. (2020b) show that for the combination of a LEIAR25.R3 LEIT antenna and a Javad receiver differences up to 2.3 mm between GL1C and EL1X and 3.2 mm between GL5X and EL5X at low elevations occur.

Additionally, the receiver itself has a small impact on the estimated PCC. This was investigated in Kröger et al. (2019) for a zero baseline configuration using one single LEIAR25.R3 LEIT antenna and two different geodetic receivers (Javad and Septentrio). Here, differences up to 1 mm for the identical GPS and Galileo signals are present. Thus, a larger study with several antenna-receiver combinations have to be carried out in order to further investigate this open issue.

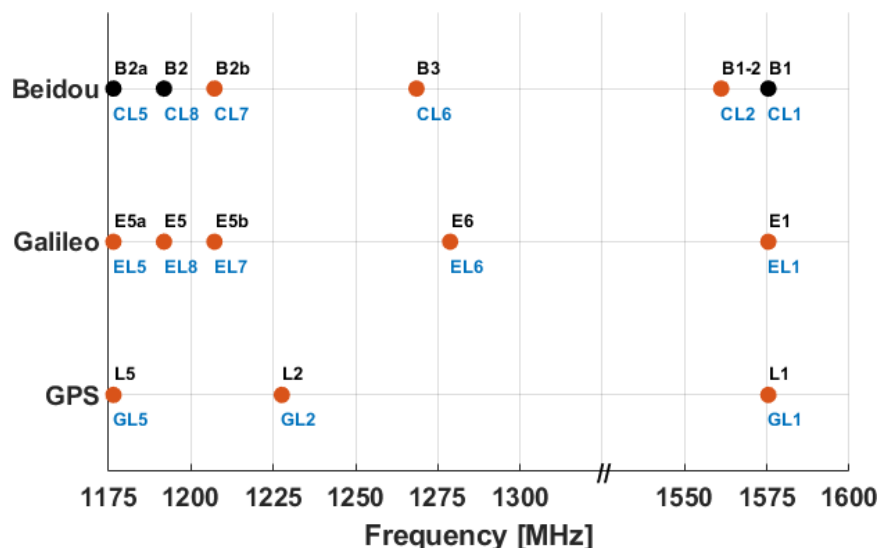


Figure 5: Representation of several GNSS frequencies. Frequencies marked in red are used in the following analyses. Black frequency specifiers name the frequency band, blue text represent the RINEX observation code neglecting the tracking mode or channel.

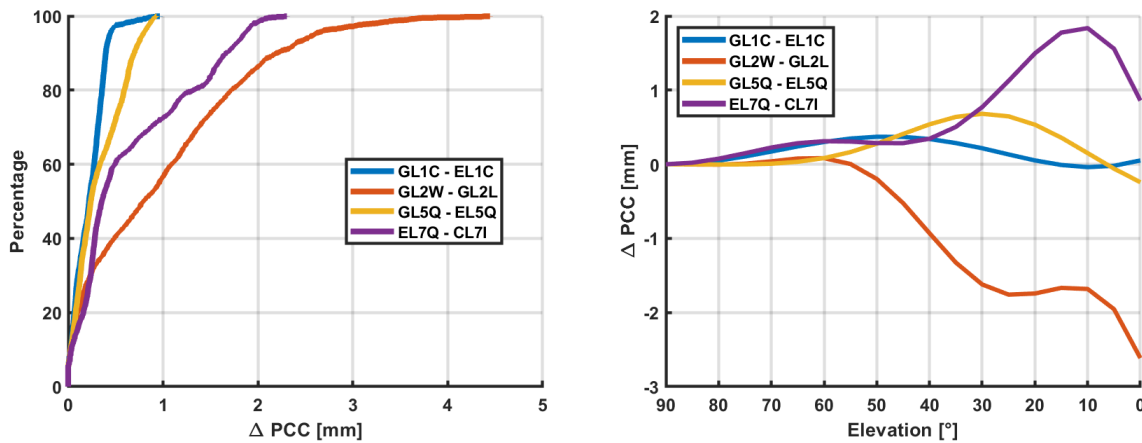


Figure 6:  $\Delta$ PCC between identical frequencies from different GNSS.

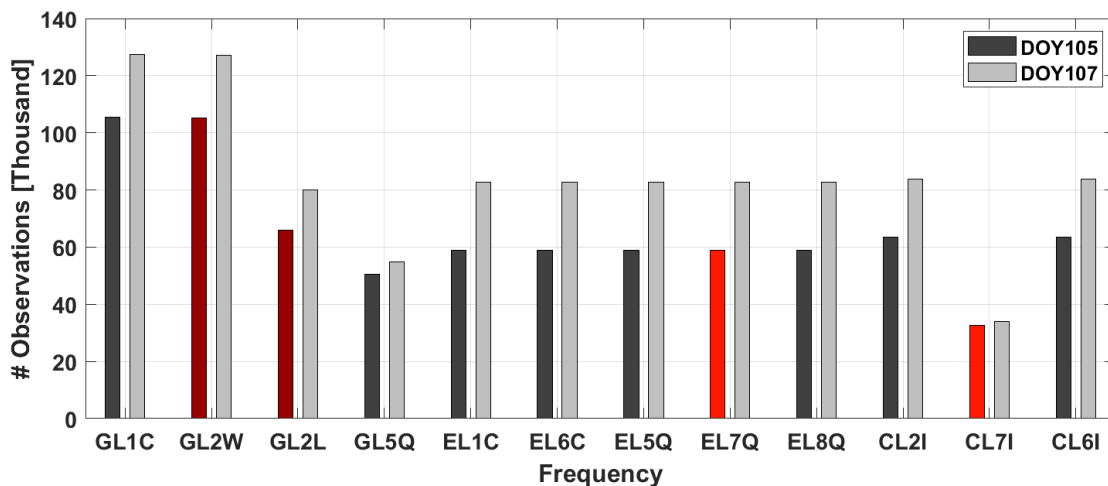


Figure 7: Total number of observations ( $dSD$ ) for the PCC estimation. One reason for higher differences between GL2W and GL2L PCC as well as EL7Q and CL7I PCC could be the significantly different number of observations.

#### 4. Joint estimation approach

Section 3 has shown that one set of PCC for identical frequencies but different GNSS could be provided for GPS and Galileo frequencies for the given antenna-receiver combination. To this end, it would be consequent to estimate the PCC in a joint estimation process. Therefore, the observations of identical frequencies from different systems (see Figure 5) have been added at the normal equation level.

Figure 8 shows the  $\Delta$ PCC between the jointly estimated PCC (denoted as L1, L5 and L7) and the individually estimated PCC, e.g. GL1C and EL1C. All differences are below 1 mm, except for the differences between L7 and CL7I. In this case, the differences reach a maximum of 1.41 mm. It is worth to note that the differences of the individual calibration to the joint estimation are smaller when more observations of that frequency were introduced in the joint estimation process. For example, 105577 GL1C and only 58840 EL1C observations are used for the joint L1 PCC estimation. Therefore, the L1 – GL1C differences are at

maximum 0.36 mm and the L1 – EL1C differences at maximum 0.62 mm. This correlation between number of used observations and differences to the joint estimation approach holds true for all investigated cases.

Compared to another antenna-receiver combination (LEIAR25.R3 LEIT-Javad) the presented differences are rather small. Kröger et al. (2020b) show that differences up to 5.52 mm for L1 – EL1C exist.

In order to have a deeper look in the impact of different number of observations on the joint estimation approach, Figure 9 and Figure 10 show the number of observations (DOY105) per 5° elevation and 5° azimuth bin. It is clearly visible that by far the most observations are available for GL1C. This is consistent with the numbers shown in Figure 7. Furthermore, it can be seen that for GL1C the most observations are present at high elevations, depicted in the center of the figures. This is due to the fact that a 18° elevation cut-off angle (topocenter) is applied during calibration to reduce multipath and that observations from a maximum of -5° in the antenna frame are included. However, the whole antenna hemisphere is covered. Since the robot poses are currently randomized but optimized for the actual GPS satellite geometry, some small 5° bins at low elevations are not covered with observations for EL1C, EL7Q and CL7I frequencies.

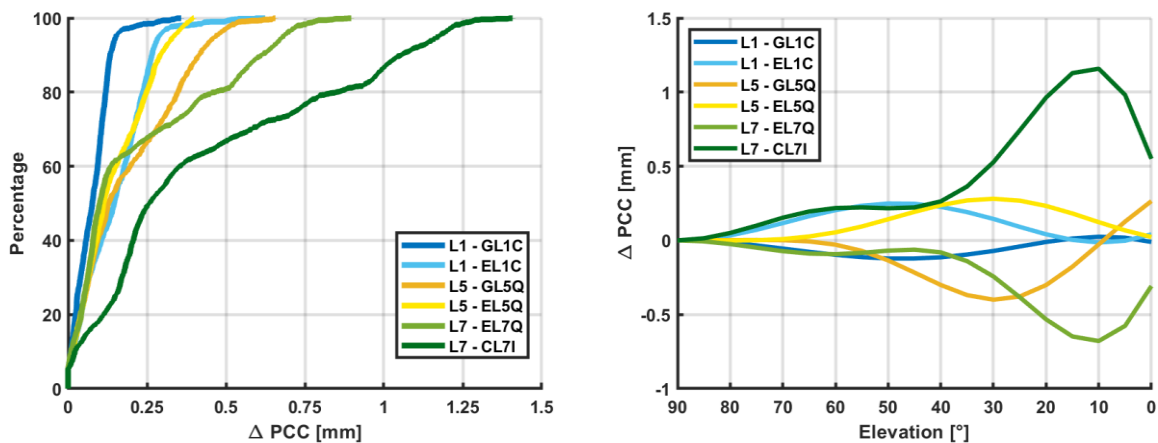


Figure 8:  $\Delta$ PCC between jointly estimated PCC (e.g. L1) and individually estimated PCC (e.g. GL1C and EL1C).

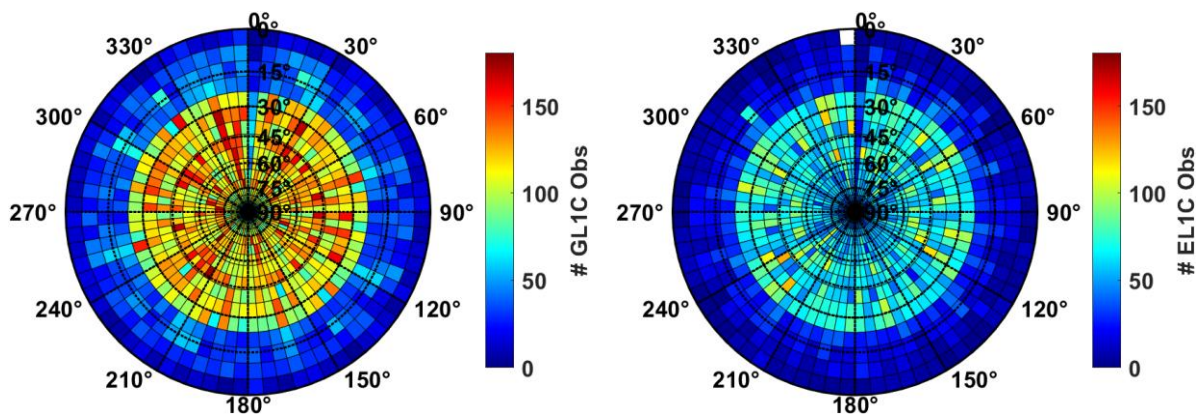


Figure 9: Number of observations for DOY105 for L1 frequencies (GL1C and EL1C).

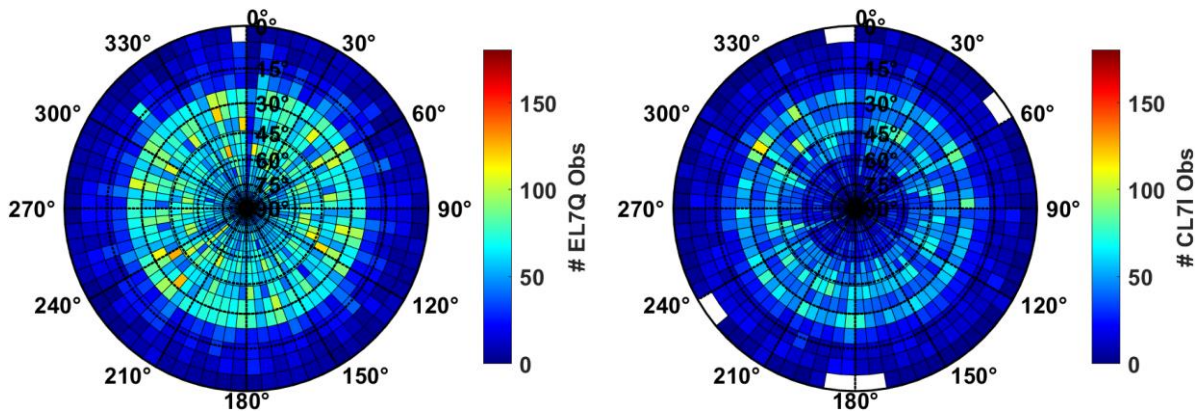


Figure 10: Number of observations for DOY105 for L7 frequencies (EL7Q, CL7I).

To finally answer the question, whether the higher differences (e.g. L1 – EL1C compared to L1 – GL1C) are caused by the different number of observations, the number of GL1C observations per 5° elevation bin was adapted to the number of EL1C observations. No adaption per 5° azimuth bin has been made since in this case the differences for the number of observations are negligible.

Figure 11 shows the number of observations per 5° elevation bin before adapting them to the number of observations of the identical frequency but different GNSS. In the case of L1, the numbers of GL1C observations are decreased per 5° elevation bin to the number of EL1C observations. Thus, the differences of the individual PCC (GL1C and EL1C) to the jointly estimated L1 PCC should be highly comparable.

Figure 12 shows the differences between the jointly estimated PCC and the individually estimated PCC with the adapted number of observations. It can be seen that the differences of the identical frequencies to the jointly estimated PCC show a more comparable behaviour than in Figure 8. Although the maximum difference decreases, the shape of the elevation dependent  $\Delta$ PCC for the L7 frequencies stays similar. Since the deviations are particularly high at low elevations, this is probably due to the rather few observations at low elevation bins, see Figure 10.

Table 3 depicts the maximal azimuthal and elevation-dependent  $\Delta$ PCC for the two investigations concerning the joint estimation process: (i) with all observations and (ii) with adapted no. of observations per 5° elevation bin for GL1C and EL7Q. Therefore, the maximal differences for these frequencies increase since less observations are used in the joint estimation process. This assumption is reinforced by the fact that the maximal differences of the EL1C and CL7I frequencies decreases as relatively more observations are contributing to the joint estimation approach. Moreover it is clearly visible, that the maximum differences between identical frequencies to the jointly estimated PCC are highly comparable. This can also be seen in the cumulative histogram depicted in Figure 12.

To summarize, the differences of individually estimated PCC to the jointly estimated PCC are mainly linked to the number of those observations that are used in the joint approach.

However, if small differences between identical frequencies of different GNSS are confirmed for further antenna-receiver combination, the joint estimation approach can boost the provision of PCC for new frequencies which are not transmitted by all satellites. As an example, by combining the observations of EL5Q and GL5Q to get a complete coverage of the antenna hemisphere before the full satellite constellation is reached. However, this should be handled carefully because otherwise one frequency would dominate the jointly estimated PCC. Thus, this only should be done for elevation bins with a low number of observations, which is mostly the case at low elevations.

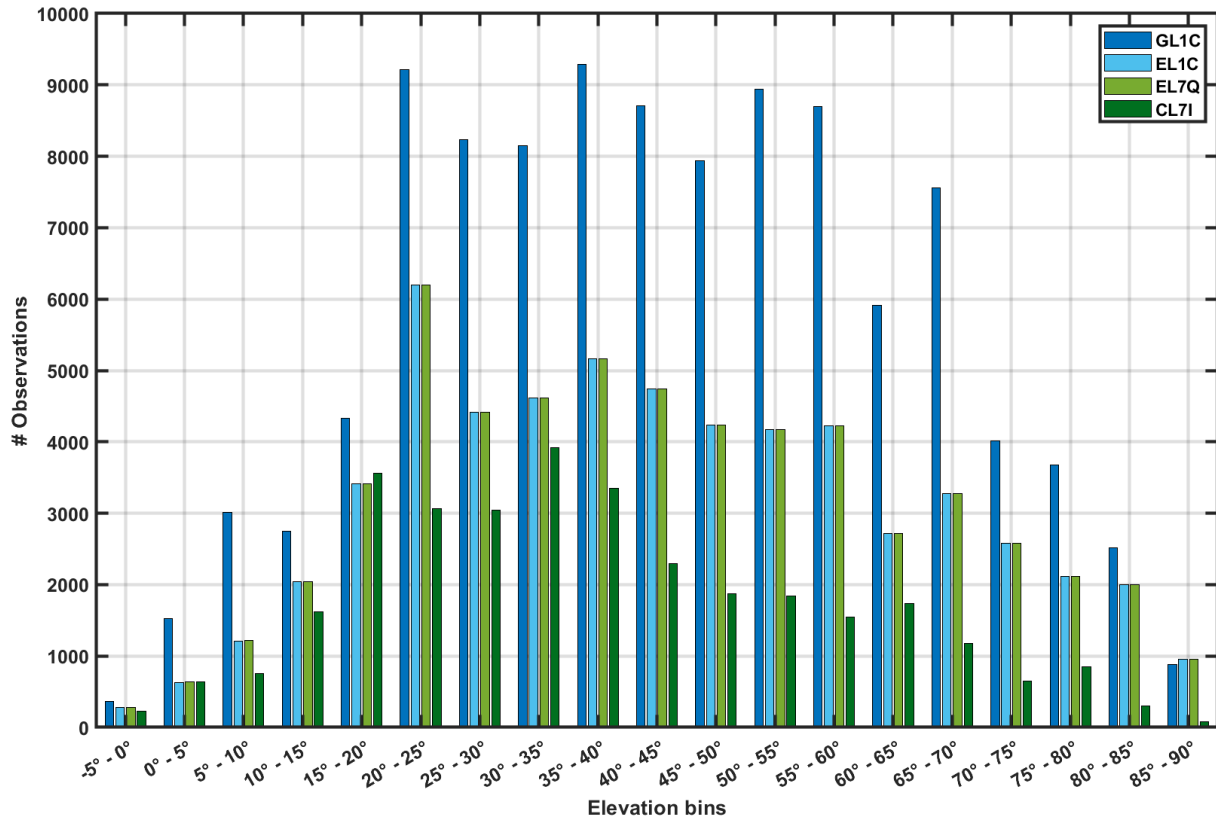


Figure 11: Number of observations per 5° elevation bin for L1 and L7 frequencies before adapting them to the identical number of observations per 5° bin.

Table 3: Maximal azimuthal and elevation-dependent APCC between individually and jointly estimated PCC taking all or the adapted number of observations as input into the estimation process.

Scenario	$\Delta(L1 - GL1C)$	$\Delta(L1 - EL1C)$	$\Delta(L7 - EL7Q)$	$\Delta(L7 - CL7I)$
All observations	0.36 mm	0.62 mm	0.90 mm	1.41 mm
Adapted no. of observations	0.54 mm	0.52 mm	1.12 mm	1.25 mm

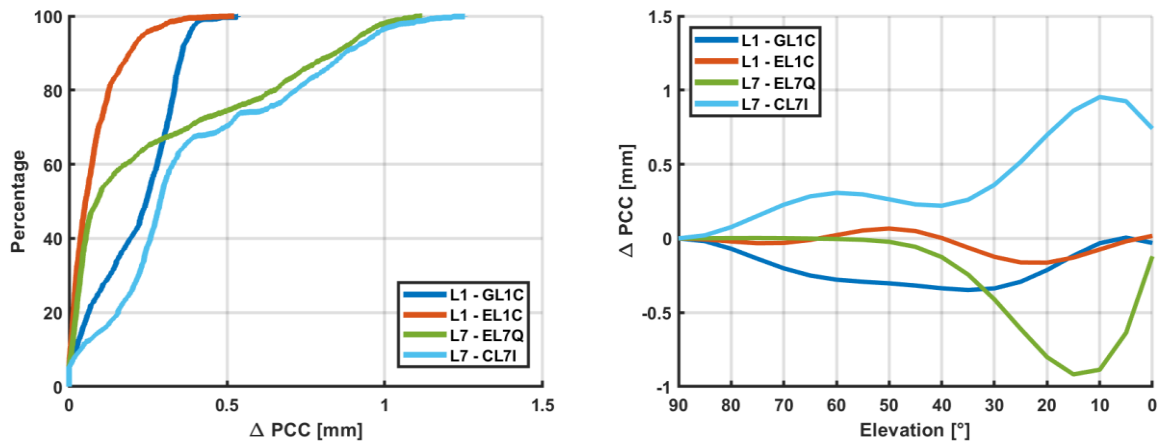


Figure 12:  $\Delta$ PCC between individually and jointly estimated PCC with adapted observation number per 5° elevation bin.

## 5. Conclusion

This contribution showed that antennas can be calibrated at the Institut für Erdmessung (IfE) with an overall good repeatability for GPS, Galileo and Beidou frequencies. The differences between two sets of PCC are at maximum of 2 mm at low elevations except for L2 frequencies of GPS. Here, the maximum is at 3 mm, probably due to the impact of tracking loop parameters on the PCC estimation.

The analyses of PCC for identical frequencies from different GNSS indicated a very good agreement between GPS and Galileo L1 and L5 frequencies below the 1 mm level. However, differences between Galileo L7 (E5b) and Beidou L7 (B2b) reached a magnitude of 2.3 mm. Here, the significantly different number of observations for the estimation process can explain these deviations.

Furthermore, an estimation approach with combined observations of identical frequencies from different GNSS showed differences to the “classical” approach smaller than 1.5 mm. When the number of observations for the joint estimation process are adapted per 5° elevation bin to the number of the other input frequency, the differences to the “classical approach” are getting very comparable, numerically at the sub-millimeter level.

All in all, the studies performed in this contribution have shown that PCC of identical frequencies from different GNSS can only be assumed to be identical to some extent.

Moreover, the presented results are only valid for the specific antenna-receiver combination and the used tracking loop parameters.

Since other antenna-receiver combinations already showed higher differences, a bigger study with several, different combinations and tracking loop parameters need to be carried out in near future in order to analyze in detail their impact on the estimated PCC.

## REFERENCES

- Altamimi, Z., Rebischung, P., Métivier, L. & Collilieux, X., 2016. ITRF2014: A new release of the International Terrestrial Reference Frame modelling nonlinear station motions. *J. Geophys. Res.*, 121(8).
- Becker, M., Zeimet, P. & Schönemann, E., 2010. Anechoic Chamber calibrations of phase center variations for new and existing GNSS signals and potential impacts in IGS processing. *IGS Workshop 2010 and Vertical Rates Symposium*.
- Böder, V. et al., 2001. How to Deal With Station Dependent Errors, New Developments of the Absolute Field Calibration of PCV and Phase-Multipath With a Precise Robot. *Proceedings of the 14th International Technical Meeting of the Satellite Division of The Institute of Navigation (ION GPS)*, pp. 2166-2176.
- Görres, B., Campbell, J., Becker, M. & Siems, M., 2006. Absolute calibration of GPS antennas: Laboratory results and comparison with field and robot techniques. *GPS Solut*, Volume 10, pp. 136-145.
- Håkansson, M., Jensen, A. B. O., Horemuz, M. & Hedling, G., 2017. Review of code and phase biases in multi-GNSS positioning. *GPS Solut*, Volume 21, pp. 849-860.
- IGS, 2018. RINEX - The Receiver Independent Exchange Format Version 3.04. *Technical Report*.
- Kaplan, E. D. & Hegarty, C. J., 2017. *Understanding GPS/GNSS - Principles and Applications*. 3. ed. Boston | London: Artech House.
- Kersten, T., 2014. Bestimmung von Codephasen-Variationen bei GNSS-Empfangsantennen und deren Einfluss auf die Positionierung, Navigation und Zeitübertragung. *Deutsche Geodätische Kommission (DGK) bei der Bayerischen Akademie der Wissenschaften (BADW)*, No. 740.
- Kersten, T. et al., 2017. Geodetic Monitoring of Subrosion-Induced Subsidence Processes in Urban Areas - Concept and Status Report. *Journal of Applied Geodesy*, 11(1), pp. 21-29.
- Kröger, J., Breva, Y., Kersten, T. & Schön, S., 2019. Determination of Phase Center corrections for Galileo Signals. *7th International colloquium on scientific and fundamental aspects of GNSS, Zurich, Switzerland*, 4.-6. September.
- Kröger, J., Breva, Y., Kersten, T. & Schön, S., 2020a. Robot-based calibration of Multi-GNSS receiver antennas using real satellite signals. *14th European Conference on Antennas and Propagation (EUCAP), Copenhagen, Denmark*, 15.-20. March.
- Kröger, J., Kersten, T., Breva, Y. & Schön, S., 2020b. Multi-GNSS Receiver Antenna Calibration. *FIG Working Week 2020, Amsterdam, The Netherlands*, 10.-14. May.
- Menge, F. et al., 1998. Results of the absolute field calibration of GPS antenna PCV. In: *Proceedings of the 11th International Technical Meeting of the Satellite Division of The Institute of Navigation (ION GPS 1998)*. Nashville, TN, USA: Institute of Navigation (ION), pp. 31-38.
- Odolinski, R. & Teunissen, P. J., 2015. Combined BDS, Galileo, QZSS and GPS single-frequency RTK. *GPS Solut*, Volume 19, pp. 151-163.
- Rao, B. R., Kunysz, W., Fante, R. L. & McDonals, K., 2013. *GPS/GNSS Antennas*. s.l.:Artech House Publishers, Norwood, USA.
- Rothacher, M. & Schmid, R., 2010. ANTEX: The Antenna Exchange Format, Version 1.4. <ftp://igscb.jpl.nasa.gov/igscb/station/general/antex14.txt>.

- Schön, S., 2007. Affine distortion of small GPS networks with large height differences. *GPS Solut*, Volume 11, pp. 107-117.
- Schön, S. & Kersten, T., 2013. On adequate Comparison of Antenna Phase Center Variations. *AGU Fall Meeting, San Francisco, California*, 9.-13. December.
- Seeber, G. & Böder, V., 2002. Entwicklung und Erprobung eines Verfahrens zur hochpräzisen Kalibrierung von GPS Antennenaufstellungen - Schlussbericht zum BMBF/DLR Vorhaben 50NA9809/8. *Institut für Erdmessung*.
- Stutzman, W. L. & Thiele, G. A., 2012. *Antenna Theory and Design*. 3 ed. s.l.:John Wiley Sons.
- Willi, D., Lutz, S., Brockmann, E. & Rothacher, M., 2020. Absolute field calibration for multi-GNSS receiver antennas at ETH Zurich. *GPS Solut*, Issue 1, pp. 24-28.
- Wübbena, G. et al., 2000. Automated Absolute Field Calibration of GPS Antennas in Real-Time. In: *Proceedings of the 13th International Technical Meeting of the Satellite Division of The Institute of Navigation (ION GPS 2000)*, September 19 - 22., Salt Lake City, UT, USA. s.l.:Institute of Navigation (ION), pp. 2512-2522.
- Wübbena, G., Schmitz, M. & Warneke, A., 2019. Geo++ Absolute Multi Frequency GNSS Antenna Calibration. *EUREF AC Workshop, Warsaw, Poland*, 16.-17. October.
- Zeimetz, P. & Kuhlmann, H., 2008. On the Accuracy of Absolute GNSS Antenna Calibration and the Conception of a New Anechoic Chamber. *FIG Working Week, Stockholm, Sweden*, 14.-19. June.

## CONTACTS

Johannes Kröger  
Institut für Erdmessung (IfE)  
Schneiderberg 50  
30167 Hannover  
GERMANY  
Tel. +49511 762 17693  
kroeger@ife.uni-hannover.de  
[www.ife.uni-hannover.de](http://www.ife.uni-hannover.de)